

Determining the Mechanism of Banxia Xiexin Decoction for Gastric Cancer Treatment through Network Analysis and Experimental Validation

Yaxing Li, Ling Li, Xue Wang, Hailiang Huang,* and Tao Han*



Cite This: *ACS Omega* 2024, 9, 10119–10131

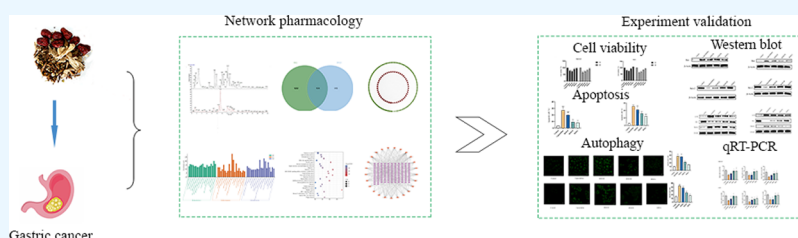


Read Online

ACCESS |

Metrics & More

Article Recommendations



ABSTRACT: Gastric cancer (GC) is a widespread malignancy. Banxia Xiexin decoction (BXD) has been used for GC treatment, but the specific mechanisms underlying its therapeutic effects remain controversial. This study used a comprehensive approach to network pharmacology combined with experimental validation to elucidate the mechanism of BXD's anti-GC effects. Initially, we used the UHPLC-LTQ-Orbitrap-MS/MS technology to identify the main chemical constituents of BXD, as well as potential targets associated with these constituents. Then, we employed the Genecard and Online Mendelian Inheritance in Man (OMIM) to determine the targets specifically related to GC. We employed a combination of Gene Ontology (GO), the Kyoto Encyclopedia of Genes and Genomes pathway, and protein–protein interaction analysis to predict the crucial targets of BXD and uncover the pathways involved in its therapeutic effects against GC. The results were subsequently verified through cell experiments. The analysis revealed 174 common targets shared by BXD and GC. GO enrichment analysis highlighted biological processes, such as autophagy, protein kinase activity, and apoptosis. Moreover, the enrichment analysis revealed several significant pathways that serve as the primary mechanisms by which BXD exerts its effects. Notably, these pathways include PI3K-Akt, HIF-1, and Pathways in cancer. Subsequent *in vitro* experiments demonstrated that BXD effectively hindered GC cell proliferation, stimulated autophagy, and facilitated apoptosis by PI3K-Akt-mTOR signaling pathway regulation. These findings reveal the effectiveness of BXD against GC through diverse components, targets, and pathways, indicating that BXD holds potential therapeutic value in GC treatment. This study uncovers the intricate biological mechanisms that underlie BXD's efficacy in treating GC through the integration of network pharmacology analysis and rigorous *in vitro* experiments.

1. INTRODUCTION

Gastric cancer (GC), which is an exceedingly prevalent and formidable malignant tumor, poses a significant global health burden, with a staggering annual incidence of over 1 million reported cases, primarily affecting Asia, Africa, and Latin America.¹ Current treatment options for GC, such as surgery, radiotherapy, and chemotherapy, have their advantages and drawbacks including patient tolerance, drug resistance, and harm to normal cells. GC ranks as the second most common cancer in China, with a significantly higher 5-year incidence compared with developed countries. The increasing occurrence of GC among younger individuals adds to the social and economic burden.² Therefore, studies focusing on low-toxicity and high-efficiency drugs for GC treatment are necessary.

The etiology of GC is multifaceted and is primarily influenced by factors such as *Helicobacter pylori* infection, lifestyle habits, dietary patterns, and familial predisposition.³ Apoptosis and

autophagy, which are distinct programmed cell death mechanisms, maintain the delicate balance of human homeostasis by facilitating self-degradation processes.⁴ Apoptosis (type I programmed cell death) encompasses distinct morphological changes, including chromatin condensation, nucleus fragmentation, cell shrinkage, and apoptotic body formations.⁵ This intricate process holds tremendous significance in the treatment and prevention of cancer and other diseases as it contributes to maintaining cellular population stability, reducing inflammatory

Received: August 25, 2023
Revised: January 18, 2024
Accepted: February 5, 2024
Published: February 21, 2024



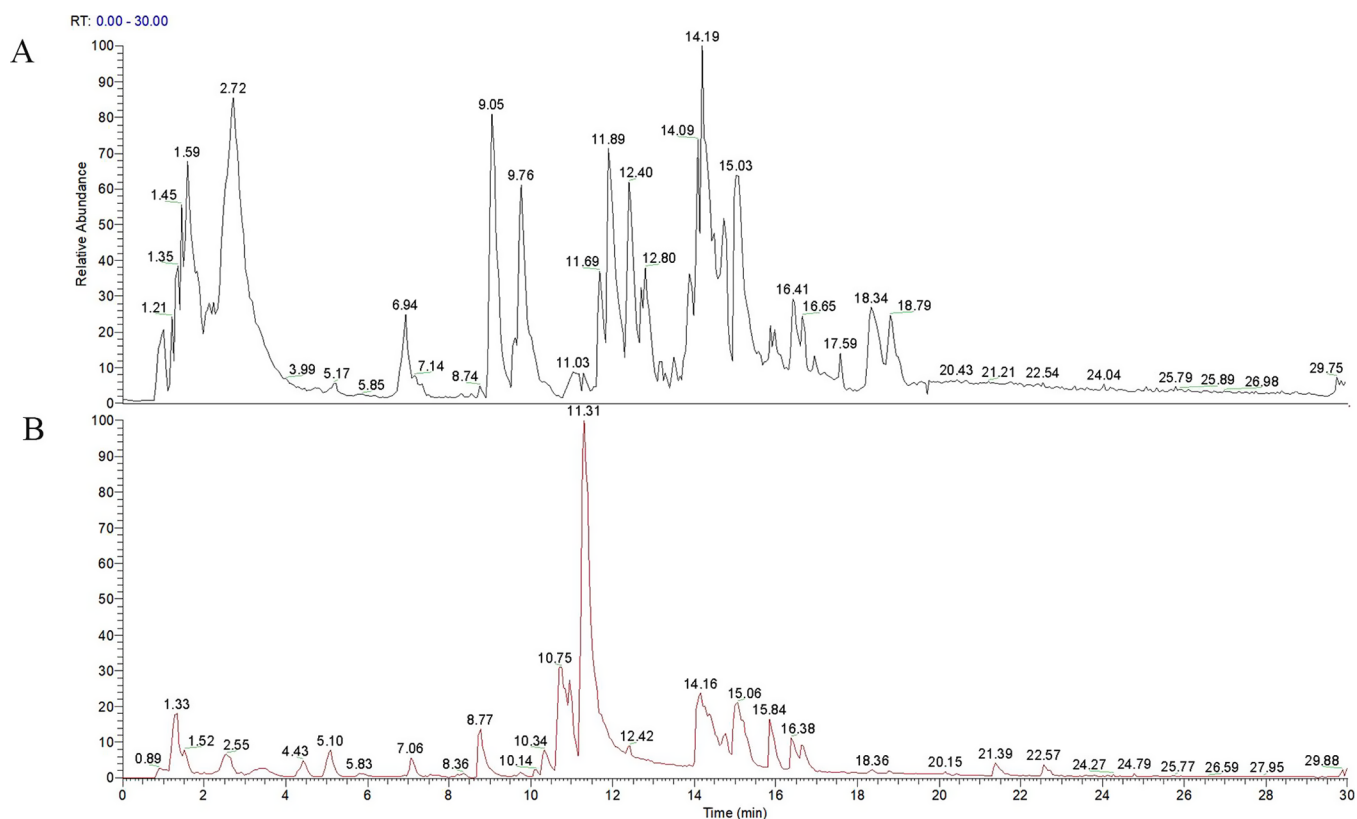


Figure 1. Identification of the chemical composition of BXD. Part A, rendered in black, signifies the total ion flow diagram in negative ion mode, whereas part B, depicted in red, represents the total ion flow diagram in positive ion mode.

responses, and eliminating damaged cells.⁶ Autophagy (autophagic/type II programmed cell death) involves cytoplasmic components and organelle self-degradation and serves a protective role in cells confronted with nutrient deficiency, oxidative stress, and pathogen infection.⁷ Autophagy and cancer have an intricate relationship, with autophagy exhibiting a dual role. Autophagy induces cancer cell death and inhibits cancer development while providing cancer cells protection.⁸ It plays diverse roles in various diseases and exhibits varying therapeutic effects on cancer. Autophagy can affect cell sensitivity to apoptosis and inhibit apoptosis.⁹ Gaining a comprehensive understanding of the intricate interplay between autophagy and apoptosis is of paramount importance in unraveling the mechanisms that underlie cancer drug treatments.

Traditional Chinese medicine (TCM) has recently garnered substantial recognition as a valuable complementary or alternative approach to Western medicine. Banxia Xiexin decoction (BXD) is composed of seven kinds of herbs: *Pinellia ternata* (Thunb.) Makino. (Ban Xia), *Coptis chinensis* Franch. (Huang Lian), *Scutellaria baicalensis* Georgi. (Huang Qin), *Zingiber officinale* Roscoe. (Gan Jiang), *Glycyrrhiza glabra* L. (Gan Cao), *Panax ginseng* C. A. Mey. (Ren Shen) and *Ziziphus jujuba* Mill. (Da Zao), the ratio of them is 2.5:1:3:3:3:2. BXD is commonly used to regulate the spleen and stomach. It significantly improves symptoms of chronic atrophic gastritis and reduces gland atrophy, intestinal metaplasia, and atypical hyperplasia of the gastric mucosa.¹⁰ BXD targets the PD-L1, HIF-1, EGFR, and TLR4 pathways, influencing GC cell apoptosis and proliferation.¹¹ Components, such as β -sitosterol, berberine, coptisine, and ginsenoside, classified based on medicinal flavor, directly or indirectly contribute to gastrointestinal disease management.¹²

Network pharmacology, which integrates multiple theories, such as systems biology, proteomics, and genomics, is crucial to understanding TCM action mechanisms through a combination of data analysis, computer simulations, and information retrieval from comprehensive databases. This approach facilitates the accurate prediction of action targets and intricate drug mechanisms of TCM compounds, thereby enabling a deeper understanding of the complex relationship between drugs and diseases. Moreover, it determines the compatibility principles of TCM components.⁴ Here, we used the power of authoritative databases renowned for their high prediction accuracy to elucidate the chemical composition of BXD. Key compounds within BXD were identified and subsequently integrated with disease databases through a meticulous screening process to predict the crucial targets associated with its therapeutic effects. A combination of enrichment analysis and experimental evidence was used to further unravel the anticancer mechanisms of BXD.

2. RESULTS

2.1. BXD's Component Analysis. Banxia Xiexin decoction was subjected to analysis utilizing UHPLC-LTQ-Orbitrap-MS/MS technology. Figure 1 elucidates the ion flow diagram from mass spectrometry for BXD, categorizing it into negative ion mode (Figure 1A) and positive ion mode (Figure 1B). This diagram encapsulates the chemical compositions of all BXD compounds. By cross-referencing standard product information and pertinent literature, 32 key components characterized by high BXD content and relevance to gastric cancer were identified, as detailed in Table 1.

Table 1. Active Components of Banxia Xiexin Decoction^a

no	name	formula	m/z	RT [min]	reference ion	source
1	adenine	C ₅ H ₅ N ₅	136.06181	4.43	[M + NH ₄] ⁺ + 1	BX,GJ
2	baicalein	C ₁₅ H ₁₀ O ₅	255.06461	14.089	[M + H] ⁺ + 1	BX,HQ
3	baicalin	C ₂₁ H ₁₈ O ₁₁	447.09109	14.158	[M + H] ⁺ + 1	BX
4	berberine	C ₂₀ H ₁₇ N O ₄	336.1225	14.623	[M + H] ⁺ + 1	HL
5	caffeic acid	C ₉ H ₈ O ₄	179.03415	7.478	[M-H] ⁻ - 1	HQ
6	citral	C ₁₀ H ₁₆ O	153.12727	10.411	[M + H] ⁺ + 1	GJ
7	citric acid	C ₆ H ₈ O ₇	191.01869	2.708	[M-H] ⁻ - 1	RS
8	dibutyl phthalate	C ₁₆ H ₂₂ O ₄	279.15884	18.367	[M + H] ⁺ + 1	GC,GJ,HQ,RS
9	eucalyptol	C ₁₀ H ₁₈ O	137.13245	10.262	[M + H - H ₂ O] ⁺ + 1	GJ
10	ferulic acid	C ₁₀ H ₁₀ O ₄	195.0652	9.432	[M + H + MeOH] ⁺ + 1	HL,
11	formononetin	C ₁₆ H ₁₂ O ₄	269.08035	13.234	[M + H] ⁺ + 1	GC,HQ
12	isoliquiritigenin	C ₁₅ H ₁₂ O ₄	257.08063	13.46	[M + H] ⁺ + 1	GC
13	linoleic acid	C ₁₈ H ₃₂ O ₂	279.23288	21.946	[M-H] ⁻ - 1	BX,GJ,HQ
14	oleanolic acid	C ₃₀ H ₄₈ O ₃	455.35275	21.707	[M-H] ⁻ - 1	DZ,GC
15	palmitic acid	C ₁₆ H ₃₂ O ₂	274.27371	14.727	[M + H] ⁺ + 1	BX,GJ,HQ,RS
16	palmitoleic acid	C ₁₆ H ₃₀ O ₂	255.23161	20.573	[M + H] ⁺ + 1	BX,DZ
17	quercetin	C ₁₅ H ₁₀ O ₇	301.03513	11.692	[M-H] ⁻ - 1	DZ,GC,HL,HQ
18	salicylic acid	C ₇ H ₆ O ₃	137.02306	12.702	[M-H] ⁻ - 1	RS,BX
19	scutellarin	C ₂₁ H ₁₈ O ₁₂	463.08664	13.141	[M + H] ⁺ + 1	HQ
20	shogaol	C ₁₇ H ₂₄ O ₃	277.17963	17.383	[M + H] ⁺ + 1	BX,GJ
21	succinic acid	C ₄ H ₆ O ₄	117.01794	2.949	[M-H] ⁻ - 1	BX,
22	thymidine	C ₁₀ H ₁₄ N ₂ O ₅	241.08273	6.366	[M-H] ⁻ - 1	BX
23	succinic acid	C ₄ H ₆ O ₄	117.01794	[M-H] ⁻ -1	[M-H] ⁻ - 1	BX
24	thymidine	C ₁₀ H ₁₄ N ₂ O ₅	241.08273	6.366	[M-H] ⁻ - 1	BX
25	thymine	C ₅ H ₆ N ₂ O ₂	127.05032	6.372	[M + H] ⁺ + 1	BX
26	wogonin	C ₁₆ H ₁₂ O ₅	285.0752	16.41	[M + H] ⁺ + 1	HQ
27	nepetin	C ₁₆ H ₁₂ O ₇	317.06564	12.563	[M + H] ⁺ + 1	RS
28	isoliquiritigenin	C ₁₅ H ₁₂ O ₄	257.08063	13.46	[M + H] ⁺ + 1	GC
29	6-gingerol	C ₁₇ H ₂₆ O ₄	277.17953	15.966	[M + H - H ₂ O] ⁺ + 1	GJ
30	baicalein	C ₁₅ H ₁₀ O ₅	271.05991	15.966	[M + H] ⁺ + 1	BX,HQ
31	nicotinic acid	C ₆ H ₅ NO ₂	124.03959	2.142	[M + H] ⁺ + 1	DZ,HQ
32	5,7-dihydroxy-2-phenyl-4H-chromen-4-one	C ₁₅ H ₁₀ O ₄	255.065	16.647	[M + H] ⁺ + 1	DZ

^aBX: *Pinellia ternata* (Thunb.) Makino. (Ban Xia), HL: *Coptis chinensis* Franch. (Huang Lian), HQ: *Scutellaria baicalensis* Georgi. (Huang Qin), GJ: *Zingiber officinale* Roscoe. (Gan Jiang), GC: *Glycyrrhiza glabra* L. (Gan Cao), RS: *Panax ginseng* C. A. Mey. (Ren Shen), DZ: *Ziziphus jujuba* Mill. (Da Zao).

2.2. BXD's Core Targets in GC Treatment. Through the comprehensive analysis of UHPLC-Q-Orbitrap-MS/MS, SwissTargetPrediction, Traditional Chinese Medicine Systems Pharmacy (TCMSP) database, and UniProt database, a total of 32 active ingredients and 687 target genes were identified. Additionally, 1456 targets associated with GC were collected from GeneCards and Online Mendelian Inheritance in Man (OMIM) databases. The comparison of drug and disease targets identified 174 key genes as potential therapeutic targets of BXD in the GC treatment (Figure 2).

2.3. Protein-Protein Interaction (PPI) Network. The collected target genes were analyzed using the string database, with a confidence value of 0.4. Cytoscape software was used to construct the PPI Network, which revealed 174 nodes and 5628 edges (Figure 3).

2.4. Gene Ontology (GO) and Kyoto Encyclopedia of Genes and Genomes (KEGG) Enrichment. GO and KEGG enrichment analysis was performed using the Metascape database to explore the biological functions of the 174 targets. The top 15 enrichments for BP, MF, and CC are visualized in Figure 4. Key processes in BP included "positive regulation of cell migration", "positive regulation of cell motility", "apoptotic signaling pathway", and "positive regulation of programmed cell death" These processes were associated with "vesicle lumen",

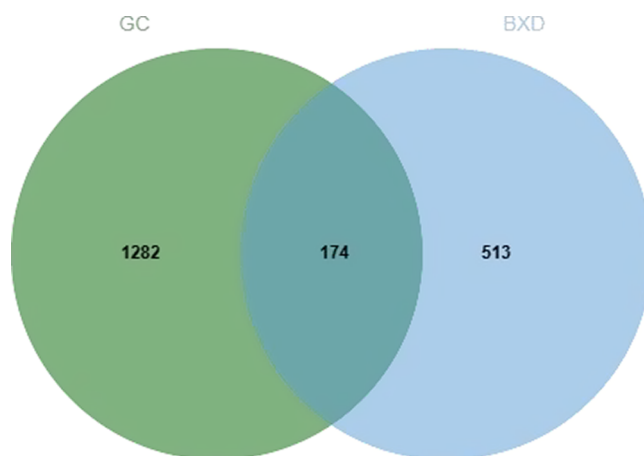


Figure 2. Banxia Xiexin decoction treatment of the GC intersection target map. GC target is indicated in green from the target of Banxia Xiexin decoction, which is highlighted in blue. GC, gastric cancer.

"apical part of cell", "receptor complex", and "apical part of the cell" in terms of GC-related CC. Significant MF functions included "protein kinase activity" and "transcription coregulator binding."

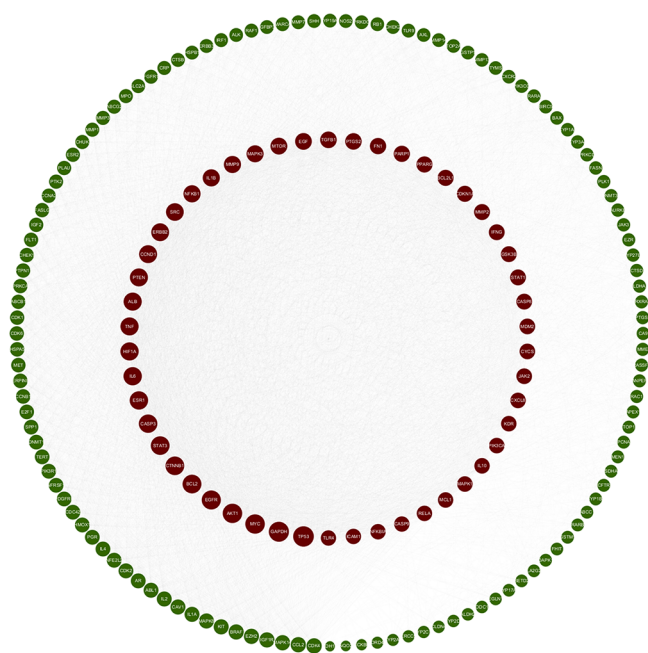


Figure 3. PPI network. PPI, protein–protein interaction. In this representation, nodes exhibit varying sizes with larger nodes indicative of higher values. As the degree value increases, the nodes transition from green to red.

We utilized KEGG analysis to predict the key pathways involved to gain deeper insights into the impact of BXD on GC (Figure 5). The figure illustrates the top 25 significant KEGG pathways associated with GC, including “Pathways in cancer”, “PI3K-Akt signaling pathway”, and “HIF-1 signaling pathway”. We constructed a disease-target pathway map to visually represent the relationship between targets and pathways (Figure 6).

2.5. BXD Inhibited GC Cell Proliferation. The inhibitory effect of BXD on MKN45 and AGS GC cell line proliferation

was investigated using different doses of BXD-containing serum (low, medium, and high). The Cell Counting Kit-8 (CCK8) assay was used for the cell viability assessment at various time points. Notably, a significant inhibitory effect was observed after 48 h of treatment, particularly with high-dose BXD. The degree of inhibition was dependent on the dose and duration, with higher concentrations and longer treatment durations resulting in stronger inhibitory effects. In contrast, the BXD low-dose group demonstrated less pronounced inhibitory effects on the MKN45 and AGS cell lines. The BXD high-dose group demonstrated significantly decreased GC cell proliferation inhibition (Figure 7). Thereafter, 48 h was chosen as the treatment duration for subsequent experiments.

2.6. BXD Promoted GC Cell Apoptosis. BXD’s effect on GC cell (MKN45 and AGS) apoptosis was examined using flow cytometry. GC cells were treated with BXD at different concentrations for 48 h, and the rate of apoptosis was assessed. The apoptosis rate of MKN45 and AGS GC cells significantly increased with an increase in drug concentration after 48 h of BXD treatment, indicating a concentration-dependent effect of BXD on GC cell apoptosis (Figure 8). Western blot was conducted to examine the effects of BXD and capecitabine-containing serum on these proteins given the involvement of various apoptosis-related proteins in the apoptotic process, including pro-apoptotic and antiapoptotic proteins. The results demonstrate significantly increased pro-apoptotic protein Bax expression with increasing BXD concentration, as depicted in Figure 8. Conversely, the expression of Bcl2, which is an antiapoptotic protein, revealed a concentration-dependent decrease in MKN45 and AGS cells, particularly with a high-dose BXD. Thus, BXD induced apoptosis, thereby affecting GC cell proliferation.

2.7. BXD Promoted Autophagy in GC Cells. MDC (Monodansylcadaverine) staining and Western blotting were used to investigate BXD’s ability to induce autophagy in GC cells (MKN45 and AGS). MDC staining evaluates how BXD influences MKN45 and AGS cell autophagy via autophagosome

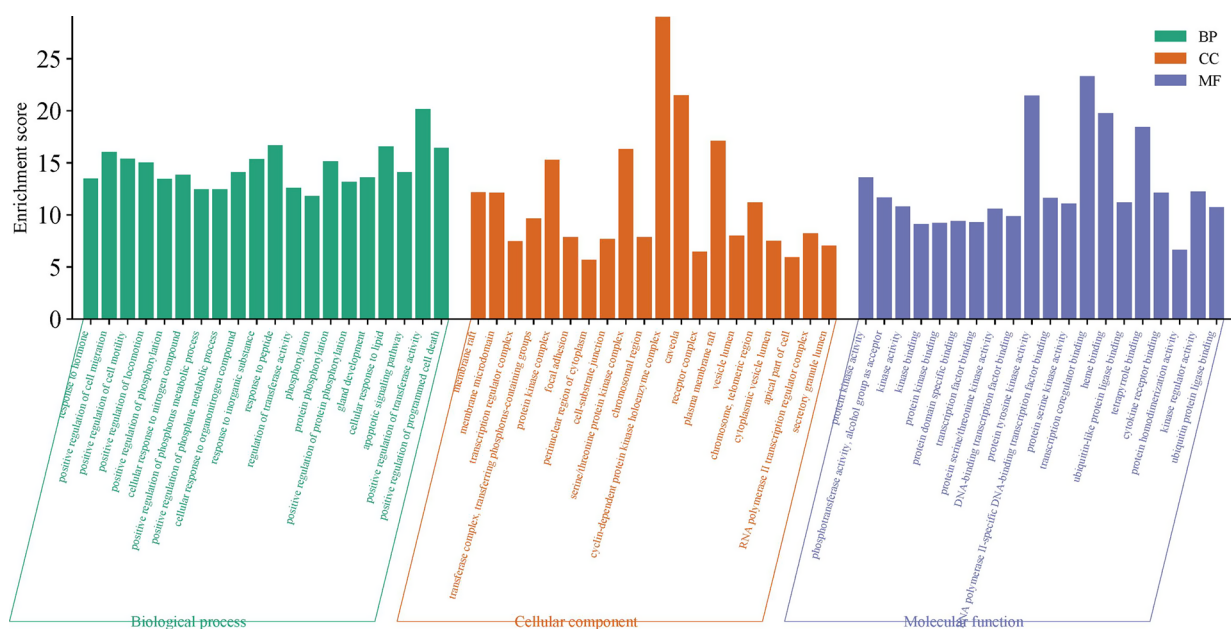


Figure 4. Enrichment analysis of GO. Green represents biological processes (BP), orange represents cellular components (CC), and purple represents molecular functions (MF). GO, gene ontology.

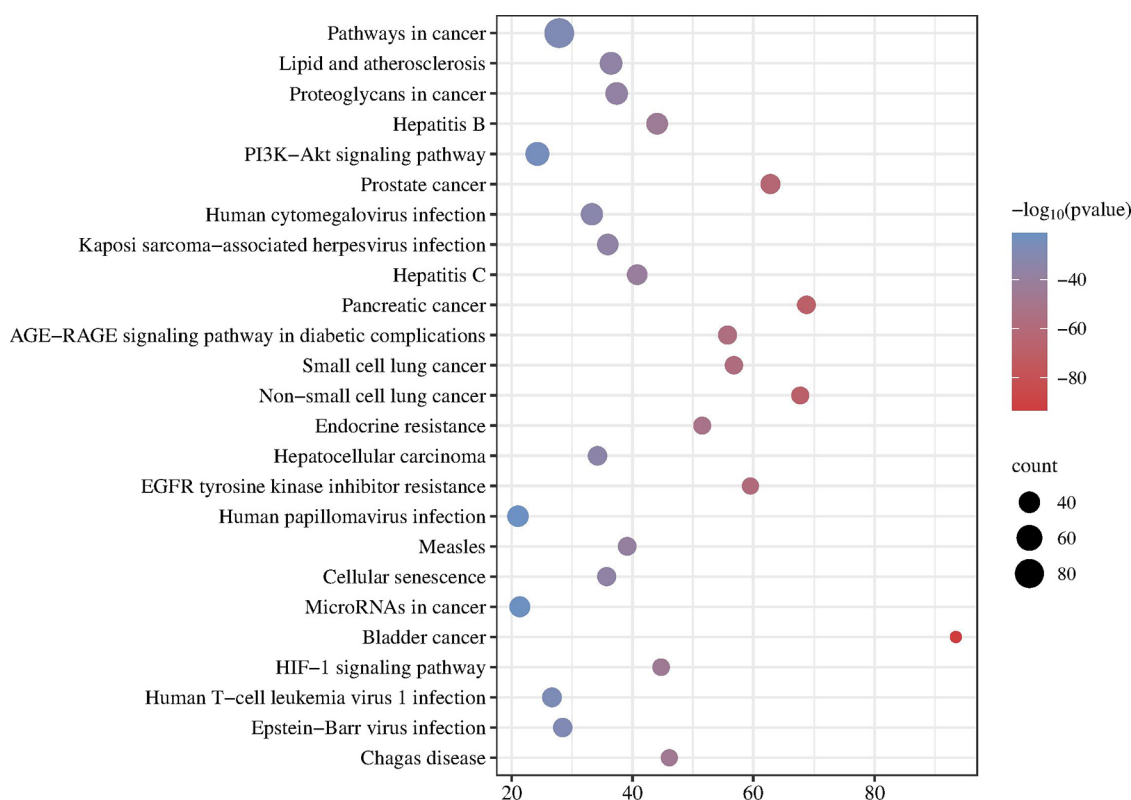


Figure 5. KEGG enrichment analysis. The larger the dot, the more relevant the genes. KEGG, Kyoto Encyclopedia of Genes and Genomes.

marker formation. MDC staining demonstrated a concentration-dependent increase in autophagosome formation in BXD-treated cells after 48 h, as shown in Figure 9.

LC3II, Beclin-1, and P62 expression levels, which are autophagy-related proteins, were evaluated using Western blot (Figure 9). A significant increase in LC3II protein expression was noted in MKN45 and AGS cells treated with varying BXD concentrations for 48 h, particularly in the high-dose group compared to the control group. Beclin-1, which is a crucial factor in autophagy initiation, exhibited increased expression levels, corresponding to the drug concentration. Additionally, P62, which is an autophagy substrate protein and autophagy indicator,¹³ demonstrated dose-dependent decreases in its concentration when treated with different BXD-containing serum concentrations. These findings indicate that BXD induces autophagy and inhibits GC cell proliferation.

2.8. Regulation of the PI3K–Akt–mTOR Signaling Pathway by BXD. qRT-PCR (quantitative real-time polymerase chain reaction) was performed to demonstrate the modulation of the PI3K–Akt signaling pathway to elucidate the molecular mechanism underlying BXD's inhibitory effects on GC cell proliferation. Figure 10 demonstrates a significant decrease in PI3K, Akt, and mTOR mRNA expression in the high-dose BXD group compared to the control group. These findings indicate that BXD regulates GC cell proliferation by modulating the PI3K–Akt signaling pathway.

3. DISCUSSION

GC, which is a malignant tumor and a leading cause of global mortality, poses a significant public health concern. The GC incidence and mortality rates in China exceed the global average.¹⁴ Unhealthy lifestyle habits, such as irregular eating patterns, increased smoking and alcohol consumption, and

excessive intake of high-salt foods, contribute to an elevated risk of GC. The disease's early detection rate is low, and mortality rates are high among patients in advanced stages despite growing awareness of GC prevention and treatment. Therefore, research efforts aim to improve early prevention, treatment, and patient survival.

TCM shows promise in cancer treatment, offering advantages over conventional Western medicine. Various forms of TCM compounds, including oral medications, granules, capsules, and injections, are commonly used in clinical tumor management.¹⁵ These compounds directly or indirectly impact tumors, thereby controlling their growth, alleviating symptoms, reducing adverse reactions, enhancing immunity, and improving quality of life.¹⁶ BXD, which is primarily used for gastrointestinal disorders, exhibits anticancer properties.¹⁷ However, the anti-GC mechanism of BXD is poorly understood. Hence, we employed a combined approach of network pharmacology and *in vitro* experiments to investigate BXD's actions against GC.

We identified 32 active ingredients and 687 target genes via the analysis of UHPLC–Q–Orbitrap–MS/MS, SwissTargetPrediction, TCMSP, and the UniProt database, respectively. Additionally, we obtained 1456 GC-associated genes from GeneCards and OMIM databases. We identified 174 shared genes as key targets of BXD in combating GC by intersecting the target genes of BXD and GC. Enrichment analysis, including GO and KEGG analyses, revealed that BXD regulates cell autophagy and apoptosis and reduces oxidative stress to improve GC development. It also affects multiple pathways, such as apoptosis, autophagy, pathways in cancer, and the PI3K–Akt signaling pathway. *In vitro* experiments corroborated these mechanisms identified through network analysis.

The CCK8 assay demonstrated dose-dependent inhibition of GC cell proliferation by BXD. Apoptosis is disrupted in cancer

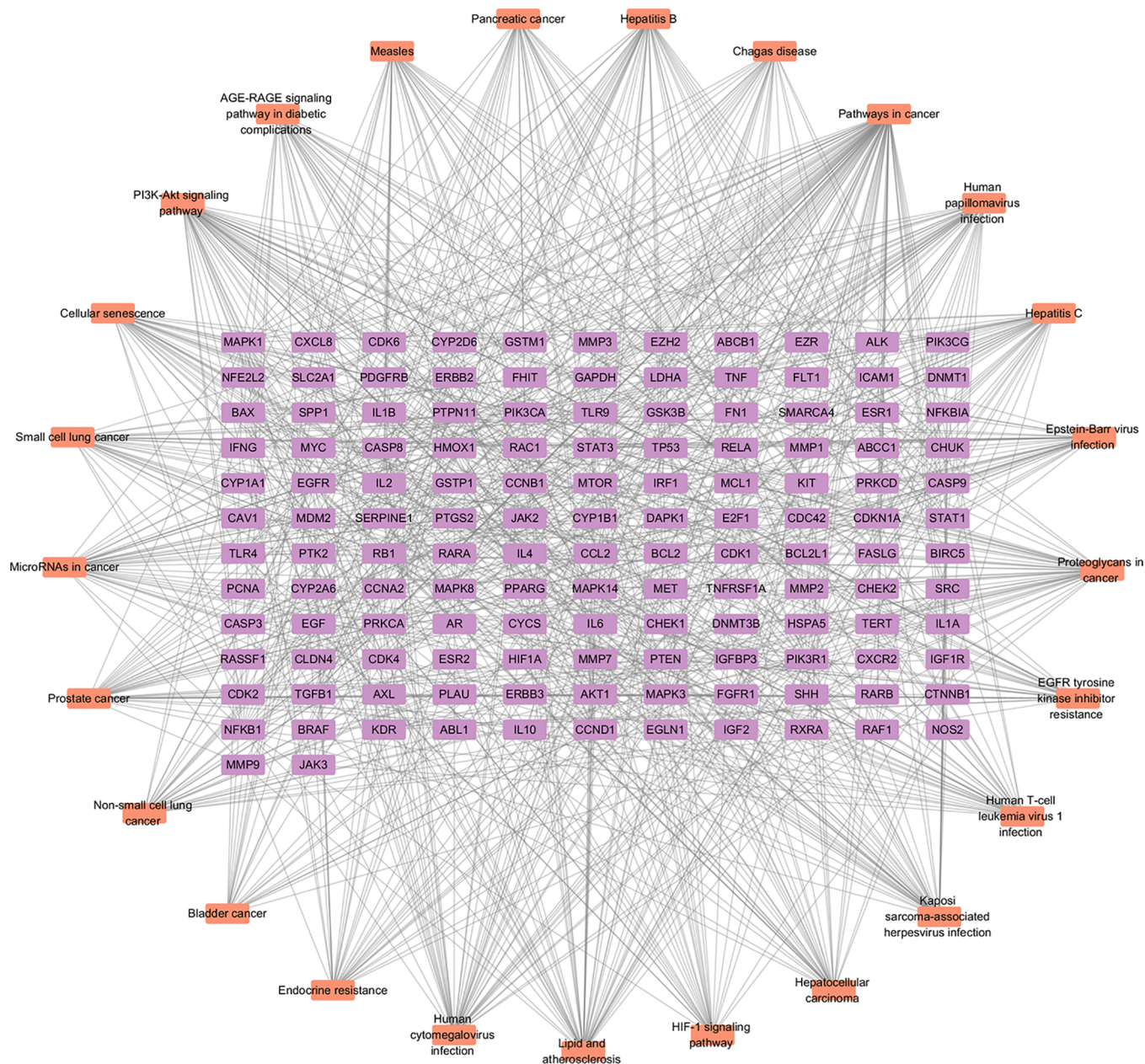


Figure 6. Component–target–pathway network. Orange nodes signify the implicated pathways, while purple nodes correspond to the targets associated with the said pathways.

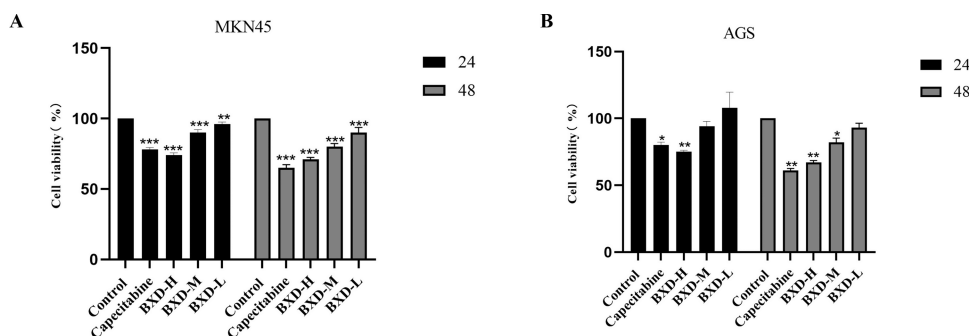


Figure 7. Banxia Xiexin decoction inhibits gastric cancer cell viability. (a, b) The survival rates of MKN45 and AGS cells were assessed after BXD-containing serum and capecitabine treatment at 24 and 48 h. compared with the control group, * $P < 0.05$, ** $P < 0.01$, *** $P < 0.001$.

cells, causing cancer cells to grow and proliferate uncontrol-
lably.⁶ Cell apoptosis is crucial in cancer. This study revealed

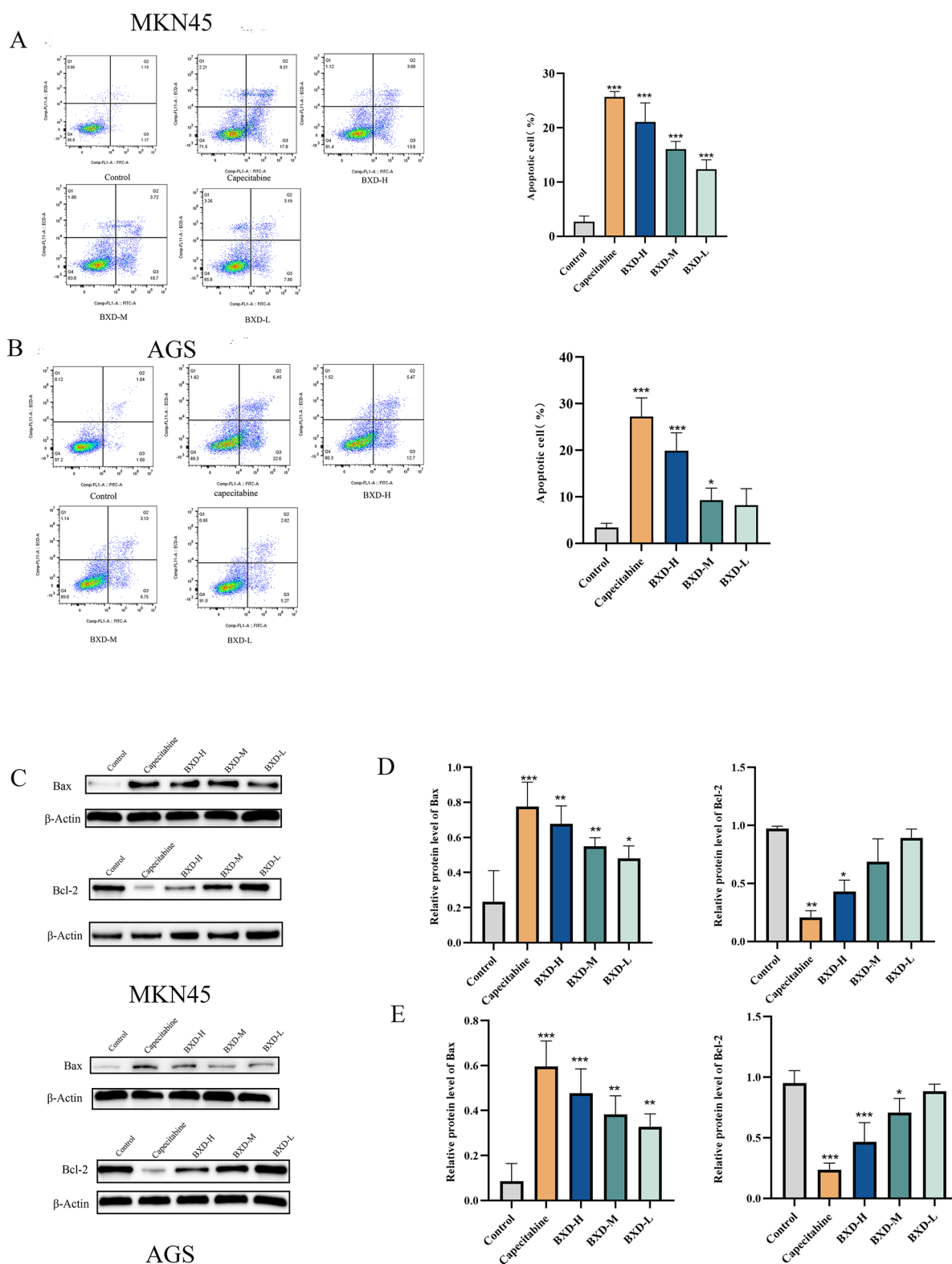


Figure 8. Apoptosis induction in gastric cancer cells by Banxia Xiexin decoction. MKN45 and AGS cells were treated with Banxia Xiexin decoction-containing serum and capecitabine for 48 h. Annexin V-FITC/PI staining was used to evaluate alterations in early and late apoptotic cells induced by Banxia Xiexin decoction and capecitabine (A, B). Expression of Bax and Bcl-2, which are apoptosis-related proteins, was examined (C). (D, E) Relative protein expression of Bax and Bcl-2. Data are shown as the mean \pm SD of three independent experiments, compared with the control group, * $P < 0.05$, ** $P < 0.01$, *** $P < 0.001$.

that BXD induces apoptosis in GC cells, with an increasing rate alongside increased drug concentration mediated by Bax and Bcl-2 protein regulation, ultimately leading to cell apoptosis.

Autophagy has different effects on tumors under different circumstances.¹⁸ On the one hand, basal autophagy is considered an important factor in inhibiting cancer develop-

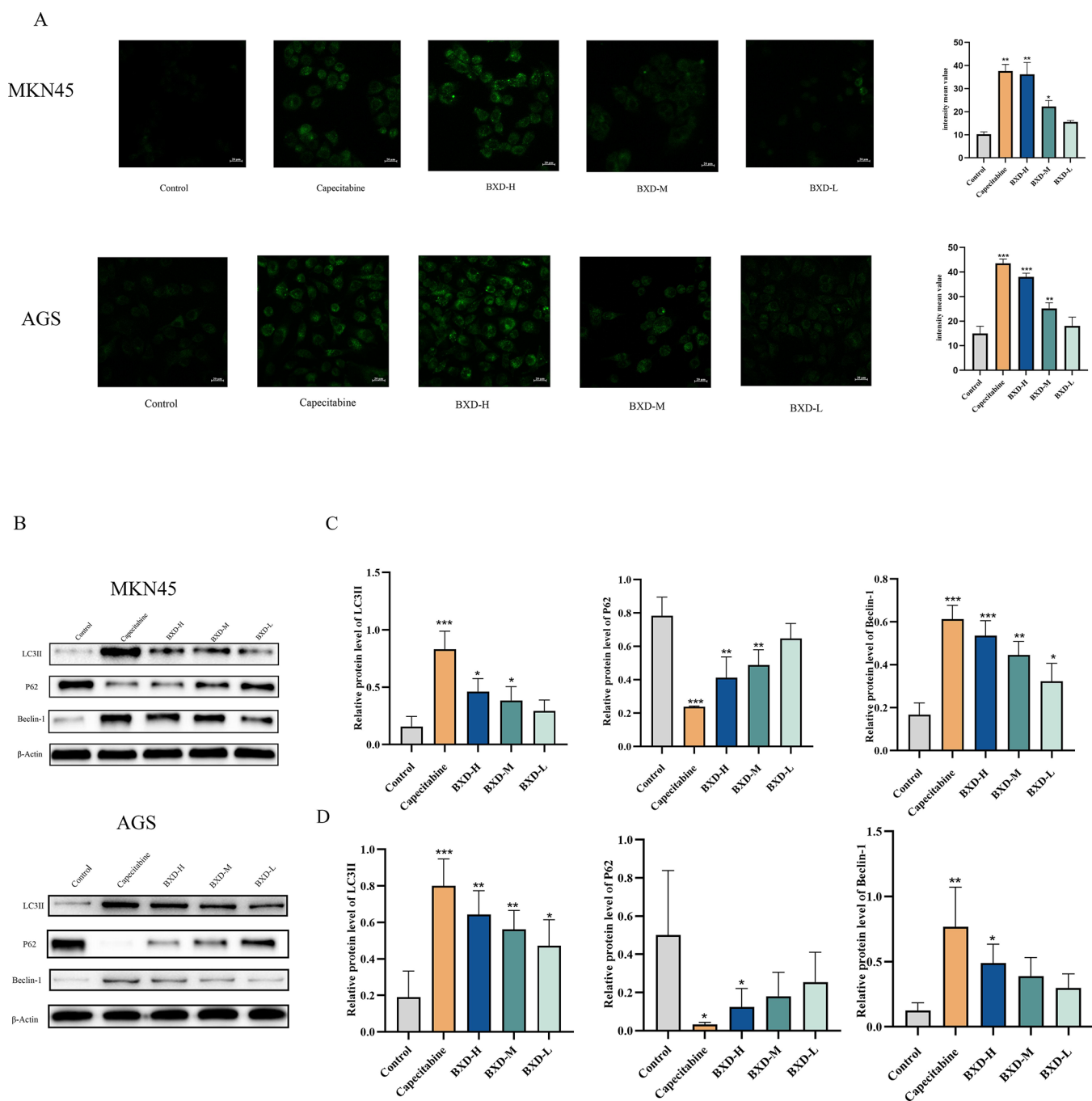
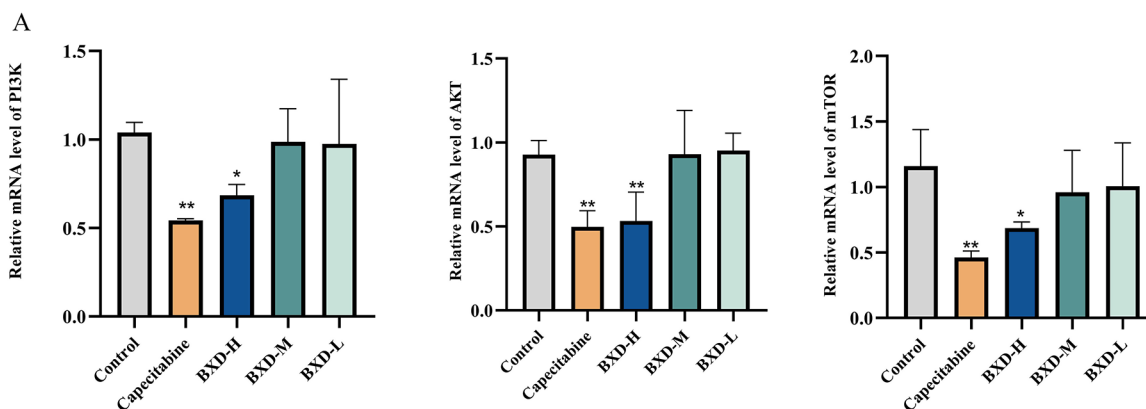


Figure 9. Banxia Xiexin decoction triggered autophagy in gastric cancer cells. (A) MDC staining was employed to determine the effect of BXD and capecitabine-containing serum on autophagy. (B) LC3II, P62, and Beclin-1 expression levels were evaluated. (C, D) Relative protein expression of LC3II, P62, and Beclin-1. Data were shown as the mean \pm SD of three independent experiments. compared with the control group, * $P < 0.05$, ** $P < 0.01$, *** $P < 0.001$.

ment, and its ability to remove damaged mitochondria can reduce reactive oxygen species production and thus inhibit tumor generation and progression.^{19,20} but on the other, autophagy can provide the required energy for tumor cells and further promote tumor development.²¹ Therefore, regulation of autophagy can be an effective strategy for cancer treatment. However, the relationship between the treatment of BXD on GC and autophagy regulation remains unclear. We hypothesize that BXD activates autophagy and inhibits GC cell development based on a combined network pharmacological analysis with experimental results. BXD's treatment with medicated serum-

stimulated autophagy, thereby increasing autophagosome accumulation within GC cells. Furthermore, the Beclin1 and LC3II expression levels were significantly increased, indicating enhanced autophagy. Conversely, the level of P62 expression significantly decreased. Beclin1, LC3, and P62 play important roles in the process of autophagy.²² Beclin-1 can regulate the formation and maturation of autophagosomes as the most important component of the PI3K–III complex.²³ Moreover, the loss of Beclin-1 can cause tumor cell proliferation as a tumor suppressor gene, thereby promoting tumor generation.^{24,25} LC3II is an autophagosome marker. It is produced by LC3-I

MKN45



AGS

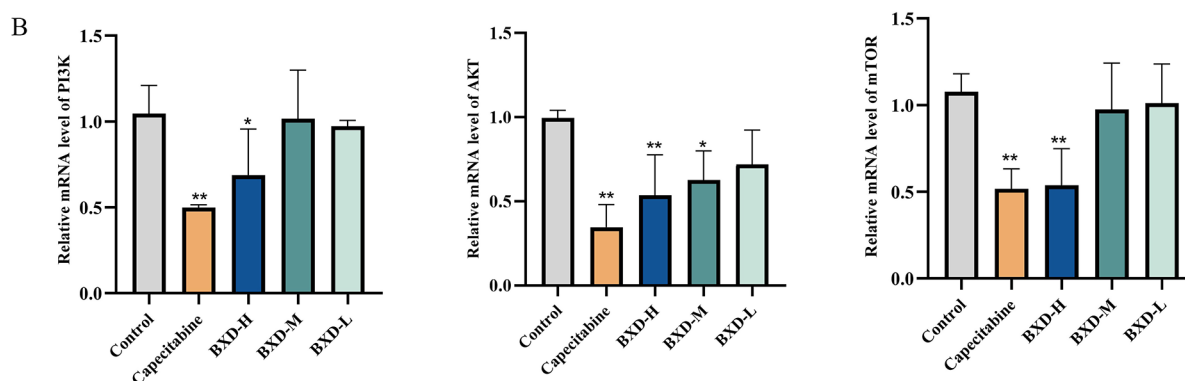


Figure 10. Impact of BXD on PI3K, Akt, and mTOR mRNA expression was assessed by using qRT-PCR. (A, B) mRNA expression of PI3K, AKT, and mTOR. Data were shown as the mean \pm SD of three independent experiments. compared with the control group, * $P < 0.05$, ** $P < 0.01$.

combining with phosphatidylethanolamine to generate lipid-soluble LC3-II, which localizes in the autophagosome.²⁶ P62 degrades protein aggregates and peroxidized substances and can be incorporated into the autophagosome only when bound to lipidated LC3B, and LC3 and P62 interact to promote autophagic degradation.²⁷

KEGG analysis revealed BXD's impact on various pathways, particularly on the PI3K/Akt/mTOR signaling pathway. This pathway regulates cell proliferation, apoptosis, autophagy, angiogenesis, and chemoresistance and is thus crucial in cancer. The mTORC1 complex, which is a component of this pathway, inhibits autophagosome generation by phosphorylating autophagy regulatory complex ULK1. Under starvation conditions, mTORC1 inactivation causes ULK1 complex activation and promotes autophagosome nucleation via PI3K/Akt/mTOR signaling pathway.^{28,29} AKT activation suppresses cell apoptosis by inhibiting Caspase-9, phosphorylating Bcl-2, and disrupting its association with the mitochondrial membrane.³⁰ Persistent PI3K/Akt/mTOR pathway activation is significant in sustaining malignant tumors. The importance of targeting this pathway in GC treatment has been established, with drugs inducing apoptosis and autophagy by modulating the PI3K/Akt/mTOR signaling pathway to inhibit cancer progression and metastasis.^{31,32} Our study reveals that BXD-containing serum significantly decreases PI3K, Akt, and mTOR mRNA expressions in GC cells. These findings indicate that BXD exerts inhibitory effects on cell

proliferation, promotes apoptosis, and induces autophagy by regulating the PI3K/Akt/mTOR pathway.

Network pharmacology, which is an advanced research tool rooted in the principles of biological network science, provides insights into intricate connections between diseases and drugs at a holistic level. The integration of network pharmacology with TCM represents a shift in TCM research from reductionism to a systemic approach.³³

4. CONCLUSIONS

In summary, we used a combination of network pharmacology and laboratory experiments to understand the effects of BXD in GC. Our findings revealed that BXD slows GC cell growth, encourages cell death, and triggers autophagy by controlling the PI3K/Akt/mTOR signaling pathway and important proteins involved in apoptosis and autophagy (Figure 11). This study provides valuable evidence supporting BXD as a potential GC treatment, highlighting the promising role of TCM in disease management. Nonetheless, it is imperative to underscore the necessity for further research concerning the pathway and the mechanistic underpinnings of Banxia Xiexin decoction in the context of gastric cancer treatment. Such investigations could be fruitfully explored through in vivo experiments, thereby affording a more robust scientific foundation for this therapeutic approach.

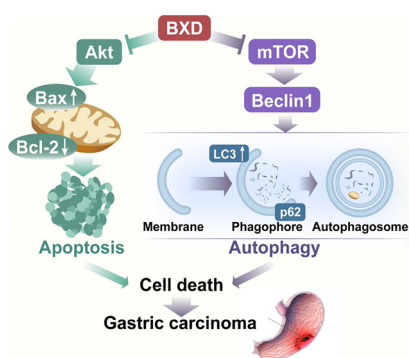


Figure 11. Diagram of the possible mechanism of action of BXD on GC.

5. MATERIALS AND METHODS

5.1. UHPLC-Q-Orbitrap-MS/MS Analysis. The chromatographic conditions employed herein are delineated as follows: the chromatographic column utilized is AQ-C18 (150 × 2.1 mm, 1.8 μm); the column temperature is set at 35 °C; the flow rate is maintained at 0.3 mL/min; and the injection volume stands at 5 μL. The aqueous phase comprises a 0.1% formic acid/aqueous solution, while the organic phase consists of methanol. Specific details regarding the gradient elution process can be found in Table 2. Mass spectrometry conditions

Table 2. Chromatographic Gradient

time (min)	aqueous phase (%)	organic phase (%)
1	98	2
5	80	20
10	50	50
15	20	80
20	5	95
27	5	95
28	98	2
30	98	2

encompass the use of an ESI source with a scanning mode encompassing both positive and negative ion scanning. The scanning range is set at 100.0–1500.0 *m/z*, the capillary temperature is sustained at 350 °C, and the spray voltage is maintained at 3.2 kV for both positive and negative modes. Nitrogen is employed as the sheath gas and auxiliary gas, with a mass fraction exceeding 99%. The sheath gas flow rate is 40 Arb, and the auxiliary gas flow rate is 15 Arb. The acquired data were initially organized utilizing CD 3.3 (Compound Discoverer 3.3) (Thermo Fisher) and subsequently subjected to comparative analysis via database retrieval (mzCloud).

5.2. Network Pharmacological Analysis. **5.2.1. Screening of Key Targets of BXD and GC.** The chemical constituents of BXD were meticulously examined through UHPLC-Q-Orbitrap-MS/MS, followed by the identification of the pertinent active compounds. These identified compounds were subsequently integrated into the SwissTargetPrediction and TCMSP database³⁴ to extract target information associated with the compounds. Subsequently, the UniProt database was harnessed to standardize and sift through their corresponding genes, ultimately establishing a compendium of targets pertaining to BXD components.

We conducted searches in the Genecard³⁵ and Online Mendelian Inheritance in Man (OMIM) databases³⁶ using the

keyword “gastric cancer” to identify GC-related targets. The resulting targets of both the drug and the disease were then compared using the online Venny mapping tool to identify overlapping targets as core targets, generating a Venny map.

5.2.2. Establishing the PPI Network. The STRING online tool was used to analyze core targets related to disease and drugs. We utilized Cytoscape software to create a visualization of the protein network. This allowed for a more intuitive analysis of the complex protein interactions.

5.2.3. Go and KEGG Enrichment Analysis. The shared genes were entered into the Metascape database, GO and KEGG enrichment analysis, to uncover the anticancer genes and signaling pathways associated with BXD. The Metascape database³⁷ serves as a comprehensive gene function annotation and analysis tool, integrating various data resources such as GO, KEGG, and STRING. It enables pathway enrichment, biological process annotation, gene-related protein network analysis, and drug analysis. We used Cytoscape software to construct a comprehensive disease-target-pathway map to elucidate the core targets and crucial pathways.

5.3. Experimental Verification. **5.3.1. Preparation of Drugs and Reagents.** BXD was formulated with 39 g of *Pinellia ternata*, 15.6 g of *Coptis chinensis*, 46.8 g of *Scutellaria baicalensis*, 46.8 g of *Zingiber officinale*, 46.8 g of *Glycyrrhiza glabra*, 46.8 g of *Panax ginseng*, and 31.2 g of *Ziziphus jujuba*. Shandong Jichengtang Chinese Herbal Medicine Co., Ltd. (Jinan, China) provided the herbal ingredients. Preparation method: The *Pinellia* was thoroughly washed seven times, while ginseng underwent a single decoction. The remaining herbs were combined in a casserole for decoction. After the residue was removed and secondary decoction was performed, the decocted medicine was divided into several parts and stored at −20 °C. Capecitabine (0.5 g tablets) was ground into a powder form and mixed to form capecitabine suspension. Fetal bovine serum and Roswell Park Memorial Institute-1640 (RPMI-1640) were procured from Gibco (Carlsbad, CA, USA). Biyuntian Biotechnology Co., Ltd. (Shanghai, China) provided autophagy staining detection, the CCK8 assay, and Annexin V-FITC apoptosis detection kits. Bioswamp (Wuhan, China) provided antibodies against bcl2, Bax, p62, LC3II, and Beclin-1. Solarbio (Beijing, China) provided the BCA protein concentration assay kits and RIPA lysates to facilitate the experimental procedures.

5.3.2. Drug-Containing Serum Preparation. Male Wistar rats, weighing approximately 160 ± 20 g and certified as specifically pathogen-free, were carefully chosen as the study subjects. Beijing Weitong Lihua Laboratory Animal Company (Beijing, China) provided the rats that were housed in a controlled environment, maintaining a temperature of 26 °C ± 2 °C, with a humidity level of 50% ± 10%. The animals were experimented at the Animal Experiment Center of Shandong University of Traditional Chinese Medicine following a thorough acclimatization period of 7 days (experimental ethics approval number: SDUTCM20210906001).

BXD (2.46 g/mL) and capecitabine suspension (41.62 mg/mL) were given to 20 rats through oral gavage, while the remaining rats received normal saline following the 7-day acclimatization period. The intragastric administration continued for 7 days, preceded by a 12-h fasting period before the final dose. Anesthesia was administered to the rats using an intraperitoneal injection of 2% pentobarbital sodium at 0.3 mL/100 g concentration. Blood was collected from the abdominal aorta following anesthesia, carefully transferred to EP tubes, and allowed to stand for 2 h. Subsequently, the tubes were subjected

Table 3. qRT-PCR Primer Sequences

primer name	forward primer (5' to 3')	reverse primer (5' to 3')
PI3K	CTACCATGGAGGAGAACC	TAATTCAGCCATTCATCCACC
AKT	CGAGTTTGAGTACCTGAAGC	CTTCCTTCTTGAGGATCTTCAT
MTOR	ATCTCCAAGATACCATGAACC	GACCTTAAACTCAGACCTCAC
β -actin	CATTCCAAATATGAGATGCGTT	TACACGAAAGCAATGCTATCAC

to centrifugation at 3500 rpm for 10 min to separate the supernatant serum. Then, the obtained serum was transferred to appropriately labeled centrifuge tubes and subjected to inactivation by using a water bath. The tubes were stored at a temperature of $-80\text{ }^{\circ}\text{C}$ to ensure preservation. The serum was thawed to room temperature and meticulously filtered to eliminate bacteria before use.

5.3.3. Cell Culture and Experimental Grouping. The Cell Resource Center of Peking Union Medical College provided the human GC cell lines MNK45 and AGS. Ham's F-12K medium with 10% fetal calf serum/1% penicillin (Hyclone, Logan, UT, USA) was used for AGS cell culture, and RPMI-1640 medium with 10% fetal calf serum/1% penicillin (Hyclone, Logan, UT, USA) for MNK45 cell culture. The experiment included five groups: control, capecitabine, low-dose BXD (serum containing 5% BXD), medium-dose BXD (serum containing 10% BXD), and high-dose BXD (serum containing 20% BXD).

5.3.4. Cell Viability Assay. The CCK-8 assay was performed by seeding approximately 5000 cells into the wells of a 96-well plate and allowing them to adhere and grow for 24 h in a $37\text{ }^{\circ}\text{C}$ incubator with 5% CO_2 to evaluate AGS and MNK45 cell viability. The old medium was carefully aspirated once the cells reached a density of 70 to 80%, and a prepared serum medium containing the respective drugs was added to the wells. Each well was added with 100 μL of the medium and further incubated for 24 and 48 h. Afterward, the plate was placed back in the incubator for 2–3 h after 10 μL of the CCK-8 solution was added to the wells. An enzyme-labeled instrument measured the absorbance (450 nm) to determine the cell viability.

5.3.5. Flow Cytometry. Flow cytometry was used to assess apoptosis induction in AGS and MNK45 GC cells by BXD. Initially, 4×10^5 cells per well were seeded in six-well plates and incubated overnight. Subsequently, they were treated with BXD and capecitabine for 48 h. The supernatant from the six-well plates was collected in centrifuge tubes, and the adherent cells were gently rinsed once with phosphate-buffered saline. The harvested cells were then delicately resuspended in 195 μL of Annexin V-FITC binding solution and then added with 5 μL of Annexin V-FITC and 10 μL of propidium iodide staining solution while gently mixing the contents. Flowio software was used for flow cytometry after the cells were incubated at room temperature for 10–20 min. The apoptosis rate was calculated by summing the rates of early and late apoptosis.

5.3.6. MDC Staining. The cells were first harvested, and then, a growth medium was added for resuspension and counting. Afterward, the samples were seeded into 12-well plates for a culture period of 48 h. Then, the medium was delicately removed from the 12-well plates. Each well was added with 1 mL of monodansylcadaverine (MDC) staining solution to visualize autophagosome formation. Then, the plates were incubated in darkness for 30 min to facilitate staining. Afterward, the MDC staining solution was meticulously extracted, and the cells underwent a gentle washing process by adding 0.8–1 mL of assay buffer to prevent any cell damage. This washing process was repeated thrice. The previous assay buffer was removed after

completing the final washing step, and 1 mL of fresh assay buffer was added to all of the wells. Autophagosome formation in the GC cells was observed under a confocal microscope.

5.3.7. Protein Expression Detection Using Western Blotting. Each group was supplemented with 200 μL of lysate-containing protease and phosphatase inhibitors, and the cells were thoroughly lysed at $4\text{ }^{\circ}\text{C}$. Subsequently, the lysed cells were collected by scraping them into 1.5 mL EP tubes. The BCA Protein Assay kit (Solarbio, USA) was used to determine the protein concentrations. SDS-PAGE was conducted, with each well loaded with 20 μg of protein for protein separation. At room temperature, blocking was executed using skim milk powder (5%) following the transfer of proteins onto a membrane. Subsequently, the membrane was subjected to overnight incubation with the desired antibody solution at $4\text{ }^{\circ}\text{C}$ with the following antibody concentrations: Bax (1:1000), BCL2 (1:1000), LC3II (1:1000), P62 (1:1000), and Beclin-1 (1:1000). Subsequent to this step, different bands were excised based on the relative molecular mass of the target protein. The membrane was incubated with diluted HRP-labeled secondary antibodies at room temperature for 1 h, and the cells were washed with PBS three times for 5 min each time to remove unbound antibodies. Finally, a chemiluminescence analyzer (TanON-S200, Shanghai) was used to detect bands, and TANON GIS software was used to quantify the gray value of the relevant band.

5.3.8. qRT-PCR for Relevant Gene Expression Detection. Trizol solution was used to extract total RNA, and the extracted RNA was utilized for cDNA synthesis using a first-strand DNA synthesis kit. The PerfectStartTM Green qPCR SuperMix kit was used for qRT-PCR. The reaction conditions involved an initial incubation at $94\text{ }^{\circ}\text{C}$ for 30 s, five cycles at $44\text{ }^{\circ}\text{C}$ for 5 s, and subsequent incubation at $60\text{ }^{\circ}\text{C}$ for 30 s. Each sample was analyzed in triplicate to ensure reliable results. The primer sequences were designed accordingly. β -actin was used as the reference gene to normalize the mRNA expression levels. The $2^{-\Delta\Delta\text{Ct}}$ method was used to measure the mRNA expression levels of each target gene. The primer sequences for the specific genes are listed in Table 3.

5.3.9. Statistical Analysis. The above-described experimental data were analyzed using Statistical Package for the Social Sciences version 21.0 software. The results are presented as mean \pm standard deviation to provide a comprehensive understanding of data variability. The comparison of measurement data across multiple groups has been executed through a one-way analysis of variance, satisfying the prerequisites of homogeneity of variance. Subsequent multiple comparisons were conducted utilizing the LSD test, while nonhomogeneity of variance was assessed via the Dunnett T3 test. A significance level of $P < 0.05$ has been established as the criterion for statistical significance.

AUTHOR INFORMATION

Corresponding Authors

Hailiang Huang – Rehabilitation Medicine and Physiotherapy, School of Rehabilitation Medicine, Shandong University of Traditional Chinese Medicine, Jinan, Shandong 250000, China; Email: 06000031@sducm.edu.cn

Tao Han – Pharmacology of Traditional Chinese Medical Formulas, College of Traditional Chinese Medicine, Shandong University of Traditional Chinese Medicine, Jinan, Shandong 250000, China; Email: ht60012002@163.com

Authors

Yaxing Li – Pharmacology of Traditional Chinese Medical Formulas, College of Traditional Chinese Medicine, Shandong University of Traditional Chinese Medicine, Jinan, Shandong 250000, China; orcid.org/0000-0003-4426-2822

Ling Li – Pharmacology of Traditional Chinese Medical Formulas, College of Traditional Chinese Medicine, Shandong University of Traditional Chinese Medicine, Jinan, Shandong 250000, China

Xue Wang – Pharmacology of Traditional Chinese Medical Formulas, College of Traditional Chinese Medicine, Shandong University of Traditional Chinese Medicine, Jinan, Shandong 250000, China

Complete contact information is available at:

<https://pubs.acs.org/10.1021/acsomega.3c06330>

Author Contributions

Y.L.: Writing - review and editing. L.L.: Carried out most of the experiments. X.W.: Writing - review and editing. H.H.: Formal analysis. T.H.: Conceptualization.

Notes

The authors declare no competing financial interest.

ACKNOWLEDGMENTS

This study was funded by the High Level Key Disciplines of Traditional Chinese Medicine Basic Theory of Traditional Chinese Medicine, National Administration of Traditional Chinese Medicine, Shandong University of Traditional Chinese Medicine, Jinan 250355, PR China and the Key Laboratory of Traditional Chinese Medicine Classical Theory, Ministry of Education, Shandong University of Traditional Chinese Medicine, Jinan 250355, PR China.

REFERENCES

- (1) Onoyama, T.; Ishikawa, S.; Isomoto, H. Gastric cancer and genomics: review of literature. *J. Gastroenterol.* **2022**, *57* (8), 505–516.
- (2) Wang, F. H.; Zhang, X. T.; Li, Y. F.; Tang, L.; Qu, X. J.; Ying, J. E.; Zhang, J.; Sun, L. Y.; Lin, R. B.; Qiu, H.; Wang, C.; Qiu, M. Z.; Cai, M. Y.; Wu, Q.; Liu, H.; Guan, W. L.; Zhou, A. P.; Zhang, Y. J.; Liu, T. S.; Bi, F.; Yuan, X. L.; Rao, S. X.; Xin, Y.; Sheng, W. Q.; Xu, H. M.; Li, G. X.; Ji, J. F.; Zhou, Z. W.; Liang, H.; Zhang, Y. Q.; Jin, J.; Shen, L.; Li, J.; Xu, R. H. The Chinese Society of Clinical Oncology (CSCO): Clinical guidelines for the diagnosis and treatment of gastric cancer, 2021. *Cancer Commun.* **2021**, *41* (8), 747–795.
- (3) Machlowska, J.; Baj, J.; Sitarz, M.; Maciejewski, R.; Sitarz, R. Gastric cancer: Epidemiology, risk factors, classification, genomic characteristics and treatment strategies. *Int. J. Mol. Sci.* **2020**, *21* (11), 4012.
- (4) Li, S.; Zhang, B. Traditional Chinese medicine network pharmacology: Theory, methodology and application. *Chin. J. Nat. Med.* **2013**, *11* (2), 110–120.
- (5) Li, P.; Dong, X. R.; Zhang, B.; Zhang, X. T.; Liu, J. Z.; Ma, D. S.; Ma, L. Molecular mechanism and therapeutic targeting of necrosis,

apoptosis, pyroptosis, and autophagy in cardiovascular disease. *Chin. Med. J.* **2021**, *134* (22), 2647–2655.

(6) Kim, C. M.; Kim, B. L. Anti-cancer natural products and their bioactive compounds inducing ER stress-mediated apoptosis: A review. *Nutrients* **2018**, *10* (8), 1021.

(7) Notte, A.; Leclere, L.; Michiels, C. Autophagy as a mediator of chemotherapy-induced cell death in cancer. *Biochem. Pharmacol.* **2011**, *82* (5), 427–434.

(8) Li, X. H.; He, S. K.; Ma, B. Y. Autophagy and autophagy-related proteins in cancer. *Mol. Cancer* **2020**, *19* (1), 12.

(9) Thorburn, A. Crosstalk between autophagy and apoptosis: Mechanisms and therapeutic implications. In *Prog. Mol. Biol. Transl. Sci.*; Martinez, A. B.; Galluzzi, L., Eds.; Academic Press, 2020; pp 55–65.

(10) Cao, Y.; Zheng, Y. X.; Niu, J. B.; Zhu, C. M.; Yang, D. C.; Rong, F.; Liu, G. P. Efficacy of Banxia Xiexin decoction for chronic atrophic gastritis: A systematic review and meta-analysis. *PLoS One* **2020**, *15* (10), No. e0241202.

(11) Feng, X.; Xue, F.; He, G. H.; Huang, S. P.; Ni, Q. Banxia Xiexin decoction inhibits the expression of PD-L1 through multi-target and multi-pathway regulation of major oncogenes in gastric cancer. *Oncotargets Ther.* **2021**, *14*, 3297–3307.

(12) Wang, W. W.; Gu, W. L.; He, C.; Zhang, T.; Shen, Y.; Pu, Y. Q. Bioactive components of Banxia Xiexin Decoction for the treatment of gastrointestinal diseases based on flavor-oriented analysis. *J. Ethnopharmacol.* **2022**, *291*, No. 115085.

(13) Jeong, S. J.; Zhang, X. Y.; Rodriguez-Velez, A.; Evans, T. D.; Razani, B. p62/SQSTM1 and selective autophagy in cardiometabolic diseases. *Antioxid. Redox Signal.* **2019**, *31* (6), 458–471.

(14) Cao, W.; Chen, H. D.; Yu, Y. W.; Li, N.; Chen, W. Q. Changing profiles of cancer burden worldwide and in China: A secondary analysis of the global cancer statistics 2020. *Chin. Med. J.* **2021**, *134* (7), 783–791.

(15) Liu, J.; Mao, J. J.; Wang, X. S.; Lin, H. S. Evaluation of traditional Chinese medicine herbs in oncology clinical trials. *Cancer J.* **2019**, *25* (5), 367–371.

(16) Wang, Y. S.; Zhang, Q. F.; Chen, Y. C.; Liang, C. L.; Liu, H. Z.; Qiu, F. F.; Dai, Z. H. Antitumor effects of immunity-enhancing traditional Chinese medicine. *Biomed. Pharmacother.* **2020**, *121*, No. 109570.

(17) Feng, X.; Xue, F.; He, G. H.; Ni, Q.; Huang, S. P. Banxia xiexin decoction affects drug sensitivity in gastric cancer cells by regulating MGMT expression via IL-6/JAK/STAT3-mediated PD-L1 activity. *Int. J. Mol. Med.* **2021**, *48* (2), 165.

(18) Xu, H. M.; Hu, F. The role of autophagy and mitophagy in cancers. *Arch. Physiol. Biochem.* **2022**, *128* (2), 281–289.

(19) Russell, R. C.; Guan, K. L. The multifaceted role of autophagy in cancer. *EMBO J.* **2022**, *41* (13), No. e110031.

(20) Yun, C. W.; Lee, S. H. The roles of autophagy in cancer. *Int. J. Mol. Sci.* **2018**, *19* (11), 3466.

(21) Jena, B. C.; Rout, L.; Dey, A.; Mandal, M. Active autophagy in cancer-associated fibroblasts: Recent advances in understanding the novel mechanism of tumor progression and therapeutic response. *J. Cell. Physiol.* **2021**, *236* (11), 7887–7902.

(22) Duan, Z. X.; Shi, Y.; Lin, Q.; Hamai, A.; Mehrpour, M.; Gong, C. Autophagy-associated immunogenic modulation and its applications in cancer therapy. *Cells* **2022**, *11* (15), 2324.

(23) Hill, S. M.; Wrobel, L.; Rubinsztein, D. C. Post-translational modifications of Beclin 1 provide multiple strategies for autophagy regulation. *Cell Death Differ.* **2019**, *26* (4), 617–629.

(24) Liang, X. H.; Jackson, S.; Seaman, M.; Brown, K.; Kempkes, B.; Hibshoosh, H.; Levine, B. Induction of autophagy and inhibition of tumorigenesis by Beclin 1. *Nature* **1999**, *402* (6762), 672–676.

(25) Qu, X. P.; Yu, J.; Bhagat, G.; Furuya, N.; Hibshoosh, H.; Troxel, A.; Rosen, J.; Eskelinen, E.-L.; Mizushima, N.; Ohsumi, Y.; Cattoretti, G.; Levine, B. Promotion of tumorigenesis by heterozygous disruption of the Beclin 1 autophagy gene. *J. Clin. Invest.* **2003**, *112* (12), 1809–1820.

(26) Lazova, R.; Camp, R. L.; Klump, V.; Siddiqui, S. F.; Amaravadi, R. K.; Pawelek, J. M. Punctate LC3B expression is a common feature of solid tumors and associated with proliferation, metastasis, and poor outcome. *Clin. Cancer Res.* **2012**, *18* (2), 370–379.

(27) Schaaf, M. B. E.; Keulers, T. G.; Vooijs, M. A.; Rouschop, K. M. A. LC3/GABARAP family proteins: Autophagy-(un)related functions. *FASEB J.* **2016**, *30* (12), 3961–3978.

(28) Han, X. J.; Goh, K. Y.; Lee, W. X.; Choy, S. M.; Tang, H. W. The importance of mTORC1-autophagy axis for skeletal muscle diseases. *Int. J. Mol. Sci.* **2023**, *24* (1), 297.

(29) Melick, C. H.; Jewell, J. L. Regulation of mTORC1 by upstream stimuli. *Genes* **2020**, *11* (9), 989.

(30) Ghoneim, A.; Said, N. PI3K-AKT-mTOR and NFκB pathways in ovarian cancer: Implications for targeted therapeutics. *Cancers* **2019**, *11* (7), 949.

(31) Han, S. H.; Lee, J. H.; Woo, J. S.; Jung, G. H.; Jung, S. H.; Han, E. J.; Kim, B.; Cho, S. D.; Nam, J. S.; Che, J. H.; Jung, J. Y. Myricetin induces apoptosis and autophagy in human gastric cancer cells through inhibition of the PI3K/Akt/mTOR pathway. *Heliyon* **2022**, *8* (5), No. e09309.

(32) Liu, Y. W.; Chen, S.; Xue, R.; Zhao, J.; Di, M. J. Mefloquine effectively targets gastric cancer cells through phosphatase-dependent inhibition of PI3K/Akt/mTOR signaling pathway. *Biochem. Biophys. Res. Commun.* **2016**, *470* (2), 350–355.

(33) Chen, M. T.; Zhong, G. F.; Liu, M. N.; He, H.; Zhou, J.; Chen, J. P.; Zhang, M. S.; Liu, Q.; Tong, G. D.; Luan, J. N.; Zhou, H. Integrating network analysis and experimental validation to reveal the mitophagy-associated mechanism of Yiqi Huoxue (YQHX) prescription in the treatment of myocardial ischemia/reperfusion injury. *Pharmacol. Res.* **2023**, *189*, No. 106682.

(34) Ru, J. L.; Li, P.; Wang, J. N.; Zhou, W.; Li, B. H.; Huang, C.; Li, P. D.; Guo, Z. H.; Tao, W. Y.; Yang, Y. F.; Xu, X.; Li, Y.; Wang, Y. H.; Yang, L. TCMSP: A database of systems pharmacology for drug discovery from herbal medicines. *J. Cheminform.* **2014**, *6*, 13.

(35) Stelzer, G.; Rosen, N.; Plaschkes, I.; Zimmerman, S.; Twik, M.; Fishilevich, S.; Stein, T. I.; Nudel, R.; Lieder, I.; Mazor, Y.; Kaplan, S.; Dahary, D.; Warshawsky, D.; Guan-Golan, Y.; Kohn, A.; Rappaport, N.; Safran, M.; Lancet, D. The genecards suite: From gene data mining to disease genome sequence analyses. *Curr. Protoc. Bioinf.* **2016**, *54* (1), 1.30.1–1.30.33.

(36) Amberger, J. S.; Bocchini, C. A.; Scott, A. F.; Hamosh, A. OMIM.org: Leveraging knowledge across phenotype-gene relationships. *Nucleic Acids Res.* **2019**, *47* (D1), D1038–D1043.

(37) Zhou, Y. Y.; Zhou, B.; Pache, L.; Chang, M.; Khodabakhshi, A. H.; Tanaseichuk, O.; Benner, C.; Chanda, S. K. Metascape provides a biologist-oriented resource for the analysis of systems-level datasets. *Nat. Commun.* **2019**, *10* (1), 1523.